Paper AAS 05-219

Solar Sail Transfer Trajectory Design and Stationkeeping Control for Missions to the Sub-L1 Equilibrium Region

Michael Lisano, *Jet Propulsion Laboratory, California Institute of Technology*
Dale Lawrence and Scott Piggott, *University of Colorado, Boulder*

15th AAS/AIAA Space Flight Mechanics Conference

Copper Mountain, Colorado January 23-27, 2005

AAS Publications Office, P.O. Box 28130, San Diego, CA 92198

AAS-05-219

Solar Sail Transfer Trajectory Design and Stationkeeping Control for Missions to the Sub-L1 Equilibrium Region

Michael Lisano[+], Dale Lawrence[*], and Scott Piggott[**]

The design of solar sail trajectories is treated, along with the associated thrust vector control history that transfers a solar-sail-propelled spacecraft, or sailcraft, from the Earth/Sun L1 libration point to a sub-L1 region nearer the Sun. A novel combination of trajectory design and optimization, and new sailcraft trajectory control methods are employed to produce minimum time transfers and robust trajectory tracking and stationkeeping. First, a trajectory to the sub-L1 region is targeted, where solar pressure and gravitational forces approximately balance. The nominal thrust vector control sequence that produces minimum final target state error for a given time of flight is generated using a first-order gradient-search optimization tool. Then, feedback control is applied to reduce trajectory-tracking errors along the transfer trajectory and to stabilize the (normally unstable) motion in the sub-L1 region, attracting and maintaining the spacecraft on a stationkeeping orbit.

Introduction: Sub-L1 Class Solar Sail Missions

The trajectory design and trajectory controllability analyses described in this paper are focused on Sub-L1 class Solar Sail missions. Particular examples of this mission class are the Geostorm[1] mission under study by NOAA, and the L1-Diamond[2] mission under study by the NASA Sun-Earth Connection (SEC) Program. The Sub-L1 class missions entail stationing one or more solar sailcraft in the vicinity of a location on the Earth-Sun line where Earth and Sun gravitation, and solar radiation pressure thrust exerted on a perfectly Sun-pointed sail, are in equilibrium. This equilibrium point is located Sunward of the Earth-Sun L1 libration point (the latter being approximately 1.5 million km from the Earth along the Earth-Sun line), hence it is called a "sub-L1" point. The exact location of the sub-L1 point depends upon the sail characteristic acceleration, which is a function of the sail optical properties, reflecting area and total sailcraft mass. Once it is at the sub-L1 point, the primary purpose of the sail-propelled vehicle or vehicles would be to provide a platform for instruments to measure and warn about solar Coronal Mass Ejection (CME) events, at a distance significantly closer to the Sun than the Earth-Sun L1 libration point.

A typical Sub-L1 class mission unfolds in a sequence of three phases, as depicted in Figure 1. The first mission phase consists of launch of the sailcraft from Earth and transfer to a halo orbit about the Earth-Sun L1 libration point. During the first phase, the propulsive sail membrane of the sailcraft is not yet deployed. As explained by McInnes[3], the pre-sail-deployment phase terminates in this L1 halo orbit (vs. proceeding directly to the sub-L1 point) as a risk mitigation: in the contingency that the sail membrane cannot be deployed (e.g. for mechanical reasons), the sensors on board the sailcraft can still be used to

[+] Group Supervisor, Jet Propulsion Laboratory, California Institute of Technology, Pasadena, CA 91107

[*] Associate Professor, University of Colorado, Boulder, CO

[**] Graduate Research Assistant, University of Colorado, Boulder, CO

monitor CME's, although with degraded warning time. The second phase starts with the deployment of the sail membrane and initiation of travel by the sailcraft along a transfer trajectory from the L1 halo orbit to the vicinity of the targeted sub-L1 point. The third phase, which includes the science phase of the mission, entails stationkeeping the sailcraft in the vicinity of the sub-L1 point, during the remainder of the mission. Controlled flight along the transfer trajectory (Phase 2) and during stationkeeping (Phase 3) is to be achieved by articulating the solar radiation pressure thrust vector in three-space (actually on a 2 dimensional submanifold, as described later), by slewing the sail membrane.

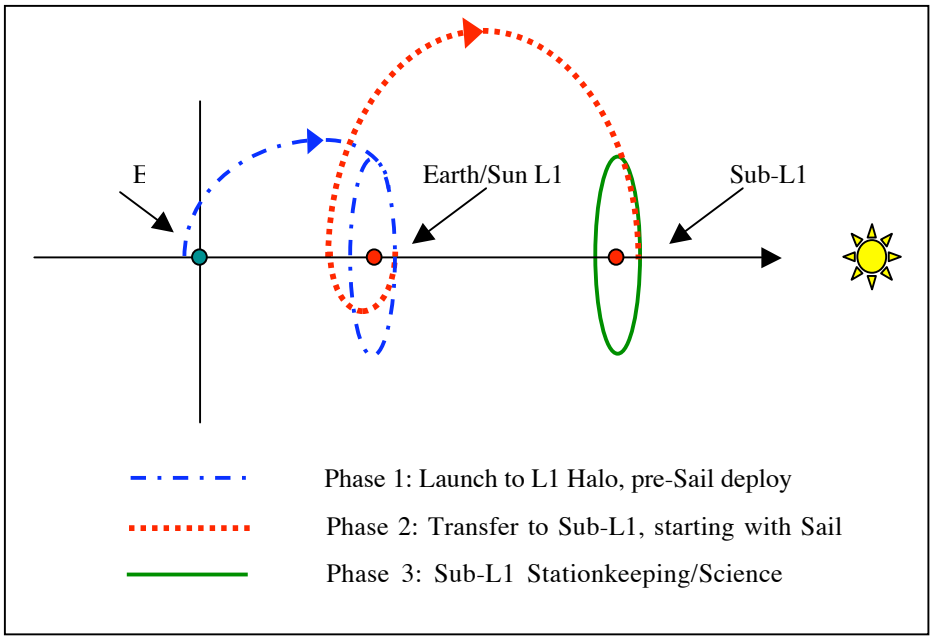

Figure 1. Sub-L1 Class Solar Sail Mission Flight Phases (Conceptual, Shown in Earth/Sun Synodic Frame)

The research reported here focuses on trajectory design and control, by solar radiation pressure thrust vector steering, for the post-sail-deploy phases, i.e. flight phases 2 and 3, of this class of mission. In particular, rapid transfer trajectories from the L1 to the sub-L1 point have been developed using a new set of algorithms being incorporated into NASA's Solar Sail Spaceflight Simulation Software[4], also called "S5", and were compared with the baseline design for the Geostorm mission. The analytical techniques have also been applied to study a variant on the Geostorm mission suggested by West[5], using updated sail materials and technologies that enable a considerably higher characteristic acceleration than what has been used in the baseline Geostorm studies to date.

L1-to-Sub-L1 Transfers Including Earth Gravity Assist

The purpose of these analyses was to explore new trajectory design and control strategies for Phase 2 and Phase 3, and compare them with the baseline Geostorm design, in particular:

- examining the possibility of shortened flight time by incorporating a "gravity assist" maneuver into the Phase 2 trajectory, by flying the sailcraft past the Earth en route to the Sub-L1 point;
- assessing the ability to control the sailcraft along the Phase 2 trajectories, correcting back to the nominal trajectory in the presence of disturbances, and
- designing and analyzing control strategies for Phase 3 stationkeeping of the sailcraft near the Sub-L1 point, based on arrival conditions from the new Phase 2 trajectories.

These analyses treat a 3-axis attitude-stabilized sailcraft with a square, 10,000 m^2 sail propulsion system, which is the baseline sail type under current study for both the Geostorm and L1 Diamond missions. Two versions of the sailcraft were analyzed; one version is the "baseline" 298-kg Geostorm sailcraft, as described by Yen (ref. 1), and the other is a 95-kg sailcraft based on updated sail membrane and boom materials and leveraging small satellite technology, as described by West[5]. The initial conditions used for these analyses were the position and velocity for a spacecraft in a halo orbit about the Earth/Sun L1 libration point. Modeling assumptions used in our sailcraft trajectory analyses are given in Table 1.

All transfer trajectories designed and analyzed here start in a halo orbit centered on the Earth-Sun L1 libration point, located approximately 1.5 million km from the Earth, on the Earth-Sun line in the direction of the Sun. The L1 halo orbit, shown in Figure 2, is roughly elliptical in shape, has a semi-major axis of approximately 700,000 km and a semi-minor axis of approximately 425,000 km, and is inclined nearly 60 degrees with respect to the ecliptic plane. Motion on this halo orbit is affected by the gravity of the Moon and Venus, as well as the Earth, and is only quasi-periodic, approximately repeating every 185 days.

The analyses in this paper begin with a baseline Phase 2 trajectory design and associated controls that were developed by Yen for the Geostorm mission. The sail controls are the cone and clock angles that orient the sail normal vector in inertial space. For the Geostorm baseline trajectory these had been designed to yield a minimum-time-of-flight transfer under the constraint that the sailcraft cone angle could not exceed 45° at any point during the transfer. The clock angle β was not constrained to any maximum or minimum value. See Figure 3 for a depiction of cone and clock angles, and how they relate to the sail normal vector and sail-to-sun vector.

Table 1. Acceleration Models Used in the Trajectory Analyses

Model	"Baseline" Sailcraft	"New Technology" Sailcraft
Sail Propulsion System	10,000 m^2, 47 kg	10,000 m^2, 43 kg
Sailcraft Payload	251 kg	53 kg
Sail Characteristic Acceleration	0.306 mm/sec^2	0.95 mm/sec^2
Gravity Model	Sun, Earth, Moon, Venus	Sun, Earth, Moon, Venus

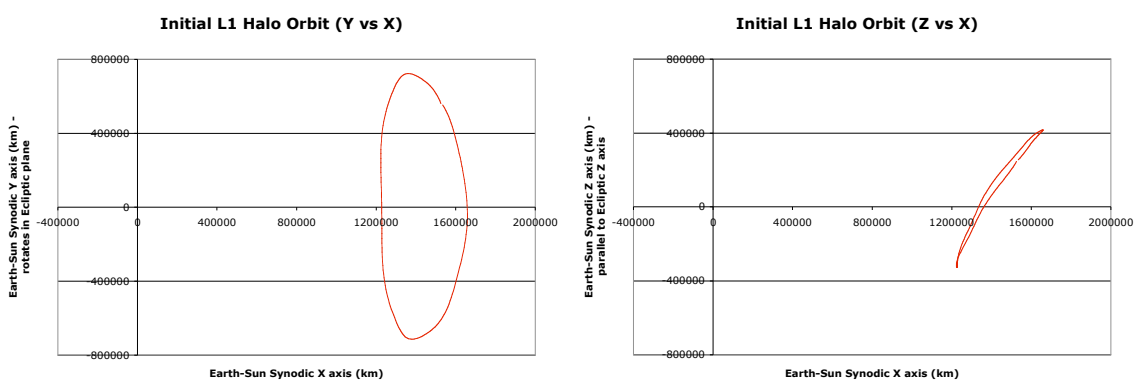

Figure 2. Initial Earth-Sun L1 Halo Orbit, Viewed in (X, Y) and (X, Z) Planes of the Rotating Earth-Sun Synodic Frame

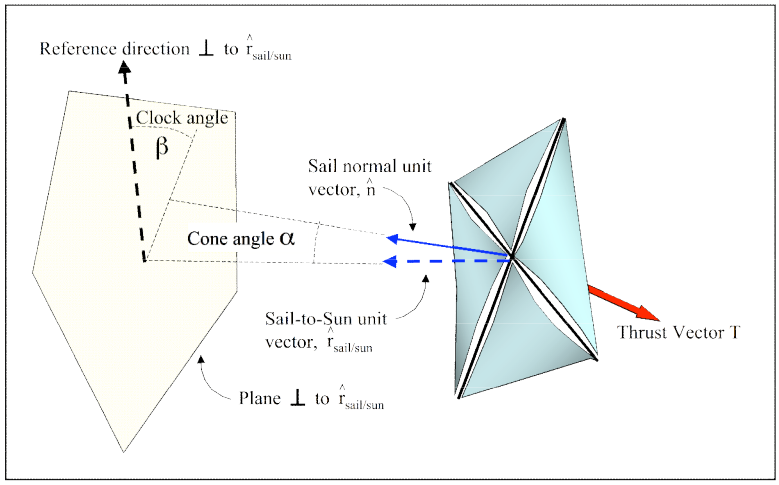

Figure 3. Sailcraft Thrust Vector Control By Steering Cone and Clock Angles of the Sail Normal

Baseline Trajectory: The baseline Phase 2 trajectory (developed by Yen) is plotted in Figure 4, along with the cone and clock angle control history. The sailcraft departs the L1 halo orbit on March 26, 2009. The cone angle is initially held at the constraint boundary of 45° for 17 days post-L1-departure, gradually flattening to 39° by day 45, while the clock angle is steered from 130° to 100°, decelerating the sailcraft in the heliocentric inertial frame, while also changing its Z-axis direction of travel from a +Z to a -Z heading. The cone angle then returns to the 45° constraint boundary by day 64, and remains at that value until day 179. During this constant-cone-angle time interval, the clock angle is steered gradually from approximately 95° to about 270°, to accelerate the sailcraft in the heliocentric inertial frame, while also changing its Z-axis direction of travel from a –Z to a +Z heading.

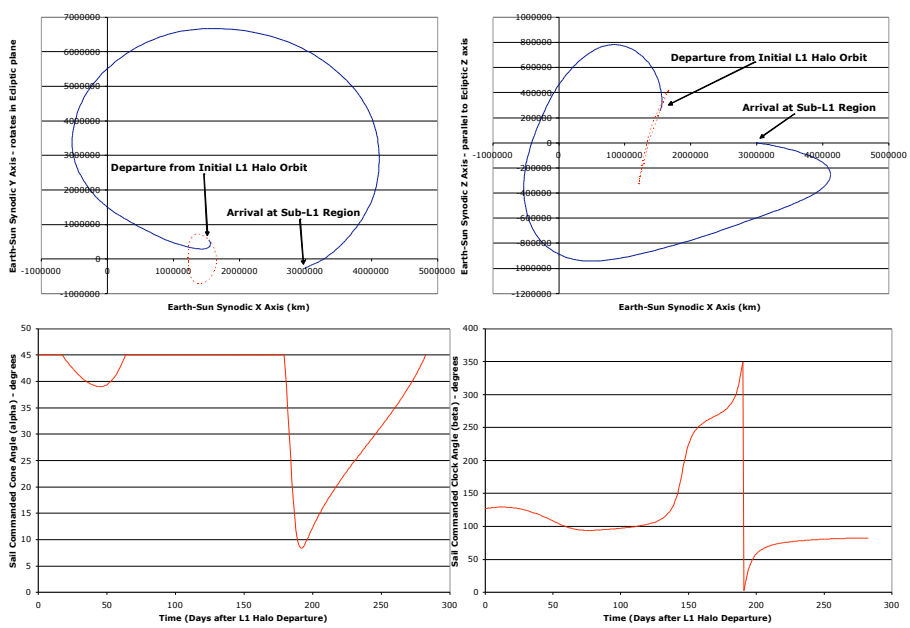

Figure 4. Baseline Geostorm 284-Day L1-to-Sub-L1 Transfer, and Associated Cone and Clock Angle Control Histories

Next, starting on day 180, the cone angle is rapidly decreased, reaching a minimum value of about 8° on day 193, in order to rapidly decelerate the sailcraft, while the clock angle is steered to initiate the final turn into its terminal approach to the targeted sub-L1 region. Finally, from day 194 until day 283, the cone angle is gradually increased to 45° while the clock angle approaches 80°, decelerating the sailcraft to a point near (about 250,000 km away from) the Earth-Sun line, at a distance of 3 million km from the Earth, which is the sub-L1 region for the given characteristic acceleration of this sailcraft (approximately 0.3 mm/sec^2).

This baseline L1-to-sub-L1 transfer trajectory has some disadvantages, from both ground operations and flight subsystems engineering points of view. In particular, the mission's "cruise" ground operations, from L1 halo departure to sub-L1 region arrival, would be about nine months long, during which time the expense of ground navigation and control teams would accumulate. Moreover, the trajectory takes the sailcraft to a maximum distance from Earth of about 7 million km, on day 173, which is more than twice as distant as the sub-L1 region where the sailcraft will ultimately operate. This large maximum Earth-to-sailcraft distance could have implications for sizing of onboard communications (and associated power) subsystems for the sailcraft. This provided some motivation in our study for examining alternative, faster transfer trajectories which did not have such large excursions away from Earth,.

"Earth-Flyby" L1-to-Sub-L1 Transfer Trajectories: To find a faster, shorter maximum-range transfer trajectory that was compliant with the 45° cone angle constraint, we developed a new class of "Earth-flyby" trajectories which would loop around the origin in the Earth-centered synodic frame, passing in front of the Earth (i.e. across the Earth's heliocentric velocity vector). It was conjectured that as the sailcraft passed near the Earth, the gravity field of the Earth would have a "gravitational assist" effect on the sailcraft, decrementing its heliocentric orbital energy and also altering its heliocentric direction of travel more rapidly than could be achieved by sail thrust vector steering alone.

In order to design Earth-flyby trajectories that could be operated robustly during the passage through the Earth-Moon system, the new trajectories were constrained to pass no closer than 80,000 km from the Earth at nearest approach. This minimum allowable Earth approach distance would place the sailcraft well above the Earth's atmosphere (assuming the exosphere extends to ~2000 km) and the outer regions of the radiation belts (out to about 10 Earth radii, or ~64,000 km)[6], and also yield minimal effects of Earth gravity gradient torques on the sailcraft attitude control system. In addition, for the L1 Halo departure dates chosen, these trajectories were allowed to pass no closer than 100,000 km from the Moon at any time.

The methodology used to design the transfer trajectories involved two steps. First, given the initial date and initial conditions for a vehicle on an L1 halo orbit, a time series of approximate cone and clock angle controls was devised by trial and error, to achieve a trajectory which passed the Earth at an acceptable distance, then went on to a region within 400,000 to 500,000 km of the targeted sub-L1 location on the Earth-Sun line. Second, a first-order gradient, backward-sweep algorithm[7] was applied iteratively, to optimize the controls so the sailcraft would arrive more nearly to the targeted terminal state (typically converging to solutions that arrive within 100,000 km RSS of the target).

Several candidate Earth-flyby transfer trajectories were developed using this new methodology. However, the remainder of this paper will focus on three trajectories of particular interest. Two trajectories, based on a baseline-technology sailcraft, having a characteristic acceleration of 0.306 mm/sec^2, are plotted in Figure 5 below. The third trajectory, for a high-performance-technology sailcraft with a characteristic acceleration of 0.95 mm/sec^2, is discussed further below.

The first trajectory, plotted in green in Figure 5, departs the L1 halo orbit on the same date as the baseline Geostorm transfer case, flying within 125,151 km of the Moon 51 days later, then reaching a perigee distance of 268,948 km 54 days past departure. It is decelerated in the heliocentric inertial frame by the Earth's gravity, and its heliocentric inertial direction of travel is rapidly changed by the encounter. The sailcraft clock angle is rapidly turned from 270° to 90° four days before the Earth encounter, so that the solar radiation pressure thrust vector acts to bend the sail trajectory towards the target point on the Earth-Sun line. It arrives within 77,220 km of the targeted sub-L1 point (which is at [3.0x10^6 km, 0.0 km, 0.0 km] with zero velocity in the Earth-centered, Earth-Sun synodic frame) 119 days after departing the L1 halo orbit.

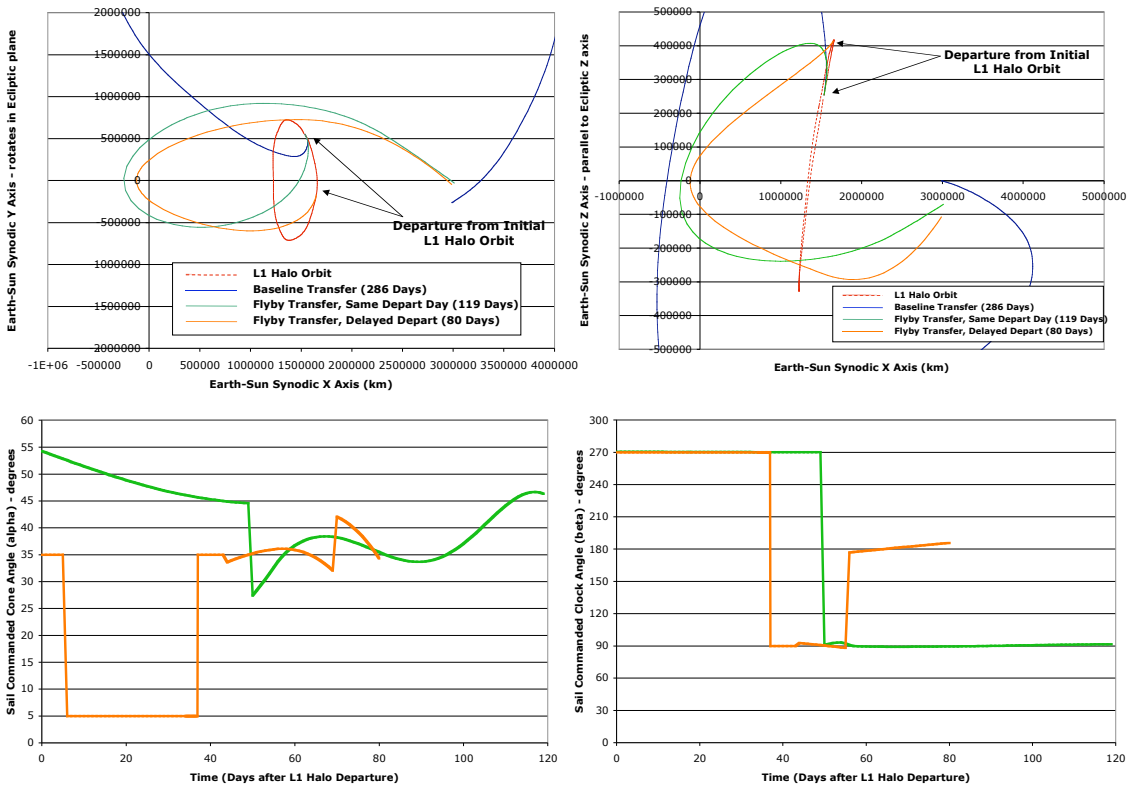

Figure 5. New "Earth Flyby"/119-Day (green) and "Delayed-Departure Earth Flyby"/83-Day L1-to-Sub-L1 (orange) Transfers, and Associated Cone and Clock Angle Control Histories

It was observed that the heliocentric inertial flight path angle of the sailcraft (as evidenced in the "kink" in the green curve shown in plot on the right side of Figure 6) is changed rapidly by the Earth flyby, which is a desired effect. But it was also noted that the orbital energy of the sailcraft in the heliocentric inertial frame was increasing dramatically in the time period between L1 halo departure and the Earth encounter (as seen in the green curve plotted on the left side of Figure 6). This occurs because the sailcraft must accelerate in order to catch up with the Earth in order to fly past and around it, as revealed by inspecting the green Earth flyby trajectory in Figure 5. Moreover, to achieve this transfer trajectory, the cone angle constraint of 45° is exceeded, reaching a maximum value of 55° in the early days of the transfer period, as shown by the green curve in the commanded cone angle plot in Figure 5.

These observations about the orbital energy and cone angle values led to a search for an alternative trajectory that would depart from the L1 halo orbit on a date later than the baseline Geostorm L1 departure date. This L1 halo departure date would be after the sailcraft (with a still-undeployed sail) had crossed the Earth-Sun line - i.e. the X axis in the Figure 5 (X, Y) trajectory plots - in order to change the geometry of the Earth approach, hopefully allowing the sailcraft to exit the Earth encounter headed more directly sunward for improved radial acceleration, and permitting a smaller cone angle throughout the transfer.

The resulting "Delayed Departure" trajectory, along with associated cone and clock angle controls, is plotted in orange in Figure 5. In this trajectory scenario, the sailcraft departs the L1 halo orbit 34 days later than the baseline Geostorm departure date, yielding a considerably different initial geometry with respect to the Earth. This different initial geometry is clearly apparent when compared with the first flyby trajectory, shown in the same plot in Figure 5. For most of the time period between L1 halo departure and the Earth flyby encounter, the sail cone angle is maintained at 5°, with a clock angle of 270°. This small cone angle nearly maximizes the solar radiation pressure thrust magnitude and directs the thrust away from the Sun, and towards the Earth. The combined effect of Earth's gravitation and the large solar radiation pressure

thrust accelerates the sailcraft to the Earth flyby, at a perigee distance of 122,595 km, 35.7 days after L1 halo departure. The sailcraft heliocentric inertial flight path angle is turned from +2° to –1.5° in about one day. Then, 37 days after L1 halo departure, the sail cone angle is increased from 5° to 35°, and the clock angle is steered from 270° to 90°, to begin a turn in the X, Y plane towards the targeted sub-L1 point. Next, 56 days after L1 halo departure, the clock angle is steered once more, to about 180°, to provide a large +Z acceleration, as the sailcraft still has a large –Z velocity component, post-flyby, and needs to be steered back towards the ecliptic plane. Using a somewhat complex cone angle steering law in the final three weeks of flight, the sailcraft arrives 118,008 km from the targeted sub-L1 point, with terminal velocity of about 1.6 km/sec in the Earth-Sun synodic frame, 80 days after having departed the L1 halo orbit.

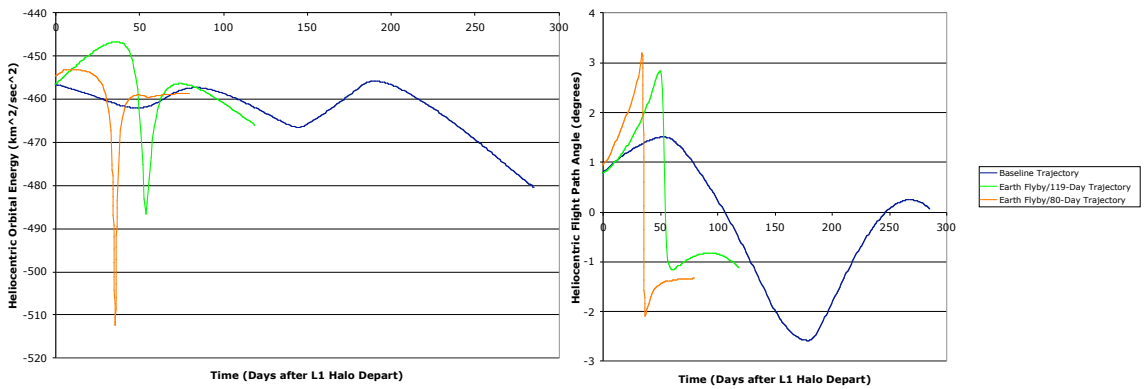

Figure 6. Heliocentric Orbital Energy and Heliocentric Flight Path Angle for Baseline Geostorm Transfer, and New Transfer Trajectories Featuring an Earth Flyby

"Advanced Technology Geostorm" Transfers With Earth Flyby: An L1-to-sub-L1 transfer trajectory with Earth flyby was also developed for a lightweight, high-performance square 10,000-m^2 sailcraft based on emerging solar sail materials and component technologies reported in a paper by West[5]. The advanced-technology sailcraft, with a characteristic acceleration of 0.95 mm/sec^2, is designed to be able to reside at a sub-L1 point 6 million km from the Earth, or twice as far from Earth as the baseline Geostorm and L1 Diamond sub-L1 point – providing a factor of four improvement in warning times for CME's, versus a non-sailcraft warning station at the Earth-Sun L1 point.

As this was a quick, initial trajectory design effort for this advanced-technology sailcraft, constraints were relaxed on both the minimum allowable flyby distance and the maximum allowable cone angle. The trajectory along with the commanded cone and clock angle histories, are shown in Figure 7 below.

Similar to the "Delayed Departure" Earth-flyby transfer trajectory described above, the "Advanced-Technology" trajectory departs from the L1 halo orbit 34 days after the baseline Geostorm departure date. The sail cone angle is initially maintained at 0° for the first 10 days to accelerate rapidly away from the Sun and towards the Earth. Then on day 10, the sailcraft cone angle is increased to 35°, with a 0° clock angle, in order to steer the sailcraft aggressively towards the perigee point. On day 20, the sail clock angle is steered to 180°, to initiate a +Z solar radiation pressure thrust acceleration component, necessary so the trajectory will curve back in the + Z direction several days after the flyby.

The sailcraft reaches a perigee distance of 67,921 km, 21.1 days after departing the L1 halo orbit. One day after the flyby, on day 22, the sail cone angle is increased again, to nearly 80 degrees, and gradually decreased in order to turn the sail back toward the Earth-Sun line in the X,Y plane. The sailcraft is then steered, following the cone and clock angle history plotted in Figure 7, arriving 73 days after L1 halo

departure at a point 90,026 km from the targeted sub-L1 point, which is at [6.0×10^6 km, 0.0 km, 0.0 km] with targeted velocity of zero in the Earth-centered, Earth-Sun synodic frame.

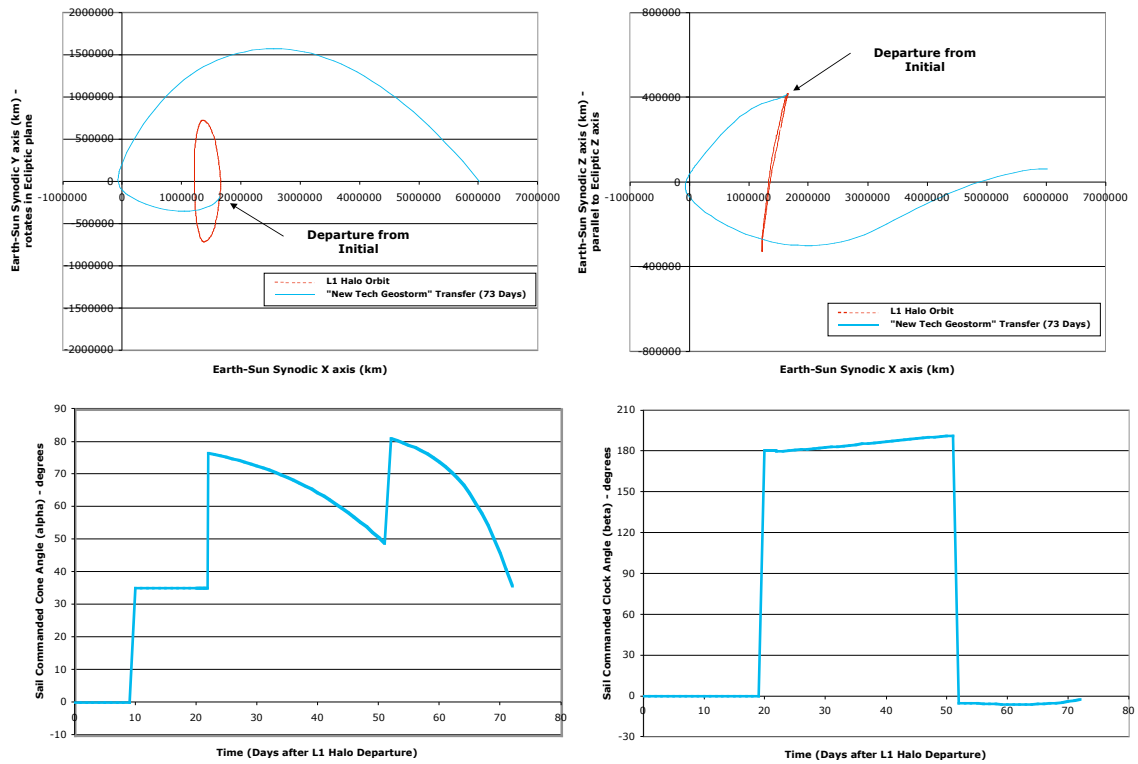

Figure 7. "New-Technology Geostorm" L1-to-Sub-L1 Transfers, and Associated Cone and Clock Angle Control Histories

Effect of Eclipses on the Trajectories: Because these trajectories were designed with a prototype for the S5 software, and an eclipse/occultation model was not yet available in the equations of motion, the effect of the sail being eclipsed from the sun by the Earth were neglected. However, a simplified occultation analysis was performed on the baseline-sail-technology, Delayed-Departure Earth Flyby trajectory, to assess the level of error incurred by neglecting eclipses while propagating these trajectories. A geometrical analysis showed that the sailcraft does, in fact, enter into the Earth's shadow for a period of approximately 57 minutes. To simulate the effect of being in the Earth's shadow, the sail was forced to have a 90-degree cone angle, and hence zero solar radiation pressure thrust, during the 57-minute eclipse period. This approximate eclipse shadow model was seen to make a 2395-km difference on the final-time state vector. This is not so large as to invalidate results discussed here, but it is an important effect that should be modeled in future studies of these transfers.

Correctability of the Earth-Flyby L1-to-Sub-L1 Transfers

In this section, we examine the relative difficulty of providing correction controls to enable the sailcraft to stay near the nominal trajectories discussed above. In the course of a mission, various disturbances will be present, causing the sailcraft to deviate from the planned trajectories. One class of disturbances are gravitational in nature, resulting from solar and planetary forces that differ from those assumed in the trajectory planning process, as well as from numerical errors produced by the discrete time trajectory propagation that underlies the iterative planning procedure. Another class of disturbances are optical in nature, resulting from uncertainties in the reflectance properties of the sail material, or from variation in sail shape or effective area relative to the (usually simple) sail model used in the planning

process. Planetary occultation, as discussed earlier, also falls in this category, as does planetary albedo. Navigation errors constitute a third class of disturbances, introducing sail angle guidance errors or mis-timed sail maneuvers due to uncertainty in sailcraft position and velocity along the intended trajectory. Fourth, disturbances are introduced by inaccurate implementation of sail angle commands by inexact attitude determination and control. Finally, atmospheric drag can occur during close planetary flybys.

While investigation of all these types of disturbances for solar sail missions is a primary goal of the S5 software, various portions are still under development. Instead, we indirectly assess the effects of these disturbances using tools from the recently developed "Trajectory Control" portion of the S5 tool set. This approach (described below) is also expected to be utilized for initial comparison of candidate trajectories in the fully developed S5 environment, since it provides a fast screening tool for making early trade-offs in mission design, saving time-consuming detailed simulations for the best trajectory candidates.

The ability of the sailcraft to correct errors away from the nominal trajectory is quantified by the system's "Correctability", defined by the development below (see the discussion in ref. 8 for more detail). We begin by placing the sailcraft translational equations of motion in state variable form

$$\dot{s} = f(s,u) \tag{1}$$

where is the state vector and the input (control) vector consists of the two angles required to specify sail normal pointing: . Here, we have used an azimuth and elevation angle relative to the Earth-Sun synodic frame, but other parameterizations (e.g. cone and clock angle) could be used instead, with appropriate changes to the function . Note that rotation of the sail about the resultant force vector does not change the accelerations applied to the sail, resulting in only two degrees of control freedom. Defining deviation variables away from the nominal trajectory, and its associated controls,

$$\tilde{s} = s - s_0 \quad and \quad \tilde{u} = u - u_0 \tag{2}$$

we obtain a linearized model at each time step along the trajectory:

$$\dot{\tilde{s}} = A\tilde{s} + B\tilde{u} \tag{3}$$

where A is the Jacobian of f with respect to s, and B is the Jacobian of f with respect to u. A "local" state variable feedback control law is designed in the form

$$\tilde{u} = -K\tilde{s} \tag{4}$$

which produces corrections to the nominal control u_0 based on off-nominal state errors $\tilde{s}$. Using this feedback law produces the following closed loop non-linear system

$$\dot{s} = f(s, u_0 - K(s - s_0)) \tag{5}$$

which can be expected to behave as predicted by the linearized design and analysis, provided that the time variations are slow compared to the specified closed loop transient responses. Detailed simulations are often needed to fully understand the behavior of this non-linear system, however, and the linearized understanding serves only as a guide.

At each time step, the controllability of the system can be examined[9,10] to determine whether transient responses can be specified as desired via placement of closed loop poles, or e.g., by Linear Quadratic optimal control. However, ability to place poles does not directly indicate how much control effort (sail

angle excursion) is needed to correct for a given off-nominal trajectory error. For this, we examine the following measure of Correctability[8].

Consider the linear system response in Eq. (3) to an initial error away from an equilibrium at $t = 0$:

$$\tilde{s}(t) = e^{At}\tilde{s}(0) + \int_0^t e^{A(t-\tau)} B\tilde{u}(\tau)d\tau \tag{6}$$

A control sequence $\tilde{u}(t)$, $t \in [0,T]$ that causes initial errors $\tilde{s}(0)$ to be corrected in a time period T, i.e. so that $\tilde{s}(T) = 0$ is given by

$$\tilde{u}(t) = -B^T e^{-A^T t} G^{-1}(T)\tilde{s}(0) \overset{\Delta}{=} H(t,T)\tilde{s}(0) \tag{7}$$

where $G(T)$ is the Controllability Gramian[10]

$$G(T) = \int_0^T e^{-At} BB^T e^{-A^T t} dt \tag{8}$$

whose inverse exists iff the pair [A,B] is completely controllable[10]. It is known[11] that this Gramian solution for $\tilde{u}(t)$ is the smallest, in the L2 sense, of all controls that can correct a given initial state to zero in time *T*. Taking the Euclidean norm of both sides of Eq. (7), we obtain the inequality

$$\|u(t)\| \le \bar{\sigma}[H(t,T)]\|\tilde{s}(0)\| \tag{9}$$

where $\bar{\sigma}[\cdot]$ is the maximum singular value. This enables a suitably small bound on the norm of the initial position and velocity errors to satisfy any desired norm bound on sail angle excursions. We can also consider initial position errors separately from initial velocity errors: Let $H_P(t,T)$ be the columns of $H(t,T)$ corresponding to the position states $\tilde{s}_P(0)$ in $\tilde{s}(0)$, and let $H_V(t,T)$ be the columns corresponding to velocity states $\tilde{s}_V(0)$. Given a desired bound D on the norm of the control deviations $\|\tilde{u}(t)\|$, the following independent bounds on initial position and velocity errors, respectively, satisfy Eq. (9), provided that the other initial errors are zero:

$$\|\tilde{s}_P(0)\| \le \frac{D}{\sup\limits_{t\in[0,T]} \bar{\sigma}[H_P(t,T)]} \quad ; \quad \|\tilde{s}_V(0)\| \le \frac{D}{\sup\limits_{t\in[0,T]} \bar{\sigma}[H_V(t,T)]} \tag{10}$$

These Correctability measures have units of [m] and [m/s], corresponding to the worst case off-trajectory errors in position and velocity that can be corrected in the time horizon , under a sail angle deviation bound .

In this paper, we use a correction time horizon of 1 day for comparing the Correctability of the nominal trajectories. This period corresponds with the discrete time update of the trajectory planning process, and may be a reasonable period to upload correction maneuvers from ground-based flight control.

A longer period could probably be used, since the length of the mission may allow larger errors than can be corrected in one day to exist in certain parts of the trajectory. In any case, the one day horizon does provide a common basis for comparison. In all cases, a sail angle excursion bound of 7.16 degrees away from nominal was used in the Correctability bounds.

Figure 8 shows the time history of the sail pointing angles, together with the position error Correctability for the baseline Geostorm transfer from the L1 halo to the vicinity of a sub-L1 station. This shows a peak daily Correctability of about 1.4×10^{-9} AU (about 200 m), and several brief periods where the Correctability dips below 1 m. The solid lines on the angle plots correspond to the cone and clock angle parameterization of sailcraft pointing from the trajectory planning results earlier. The dotted lines are the corresponding "actual" angles produced by a feedback control system (in the form of Eqn. 5) attempting to follow the nominal trajectory. Disturbances are present in this controlled simulation, relative to dynamics assumed in the planning process, in the form of neglected gravitational forces (no Venus or Moon), in the use of a different numerical integrator, and in the numerical errors caused by propagating the trajectory in the Earth-Sun synodic frame, rather than in the inertial frame. The sail reflectance model was identical to that used in trajectory planning. Figure 9 shows the resulting position and velocity in the Sun-centered Earth-Sun synodic frame, both for the nominal trajectory (solid lines) and for the "actual" trajectory produced by the daily feedback control corrections. Note that the trajectory deviations are quite large here relative to the predicted Correctability. This is because the feedback control used in the simulations has rather small gains, and the sail reacts more slowly to errors than the energy-optimal control (Eqn. 7) would. Unfortunately, this is necessary due

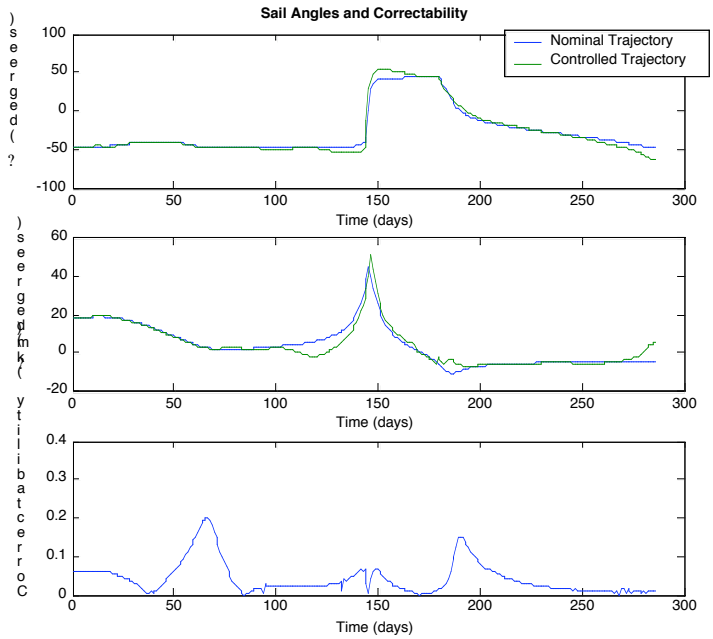

Figure 8: Sail angles and Correctability for the Geostorm baseline trajectory.

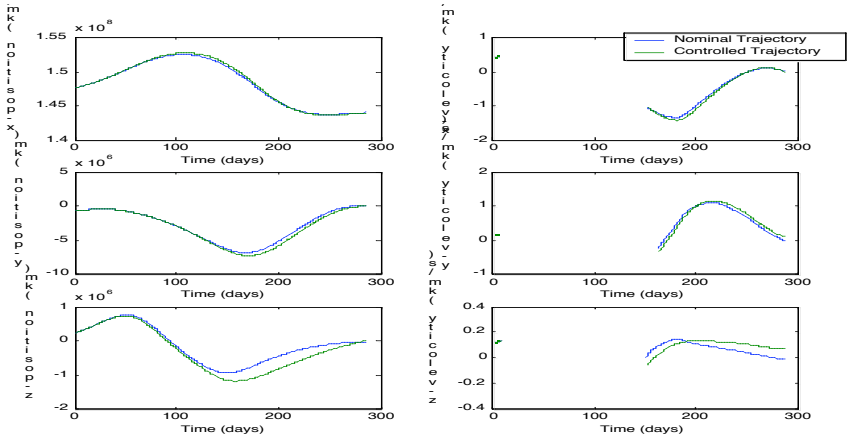

Figure 9: Position and velocity states for the nominal and feedback-corrected Geostorm trajectory.

to the size of the disturbances present in the simulation, otherwise the sail angles become too large. Despite these difficulties, the sail is able to meet the nominal terminal state with small enough error to enable capture into a stationkeeping orbit (shown later).

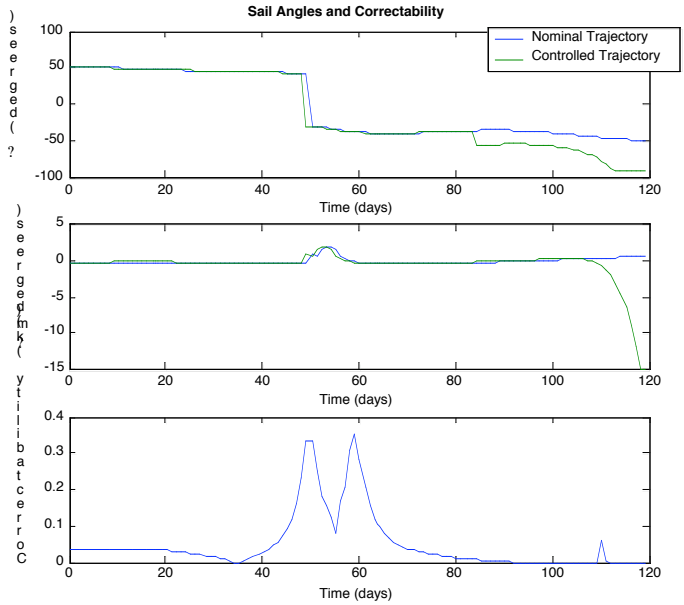

Figure 10: First Earth flyby trajectory Correctability.

The first Earth flyby trajectory has sail angles and position Correctability shown in Figure 10. This trajectory has somewhat larger peak Correctability than the Geostorm case, but suffers from very low Correctability for an extended period near the end of the trajectory. The corresponding behavior under feedback control (dotted lines) requires excessive sail angle corrections near the end. Figure 11 shows the corresponding sailcraft states. Although tracking behavior remains good, it comes at the cost of large sail angle corrections.

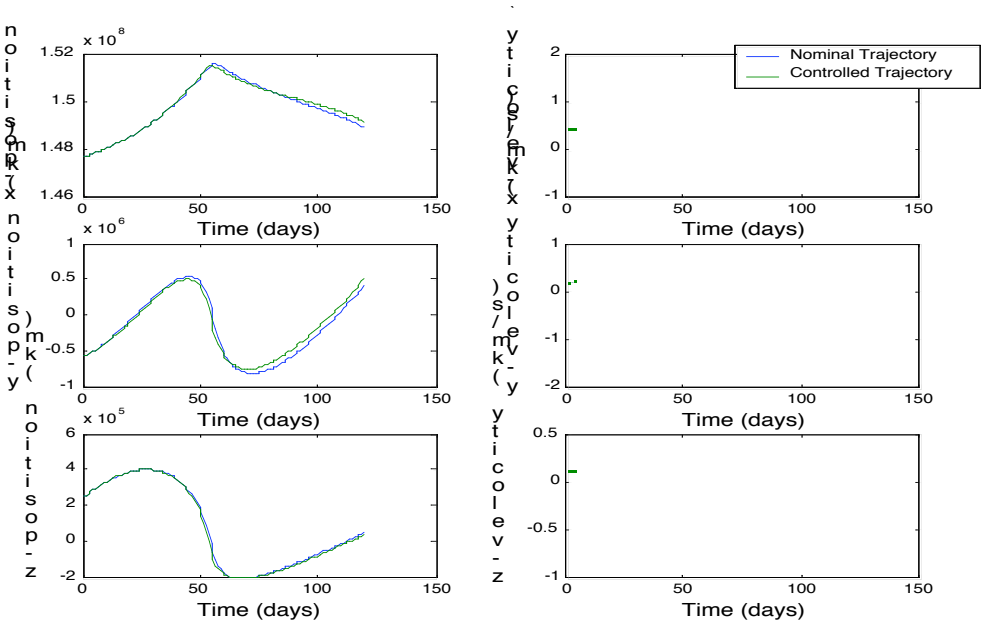

Figure 11: Sailcraft state trajectory for the first Earth flyby case.

The corresponding results for the "Late Departure" trajectory are shown in Figures 12 and 13. Prior to the true departure at about 32 days, the sail was oriented edge-on to the sun by setting the azimuth angle at 90 degrees. This trajectory seems to have a similar lack of Correctability near the end, but is actually much better than the previous case (note the larger plot scale). The initial 180 degree changes in controlled sail angles are an artifact of the controller operating in a position of no net irradiance force on the sail, and should be ignored. Otherwise, the sail angles under control remain in close proximity to the nominal ones out to the terminal time. Compared to Figure 11, the state trajectory in this case (Figure 13) shows similar tracking of the nominal, although the end state error in Z is somewhat larger.

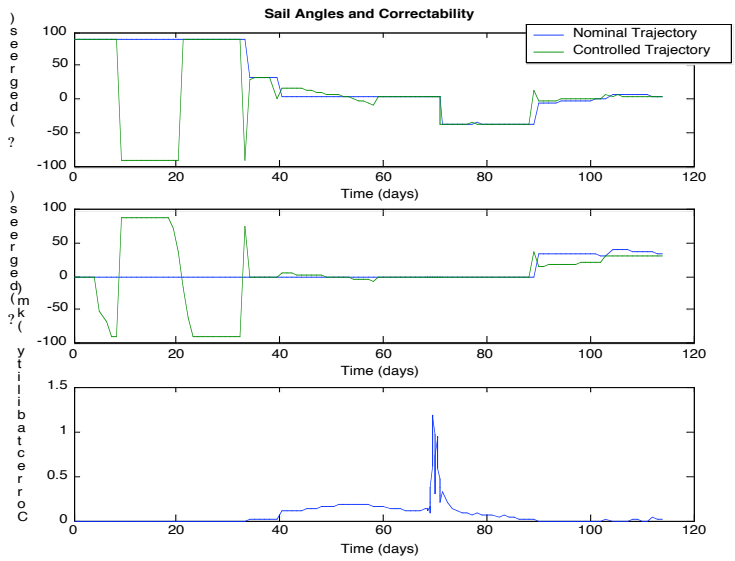

Figure 12: Late Departure trajectory Correctability.

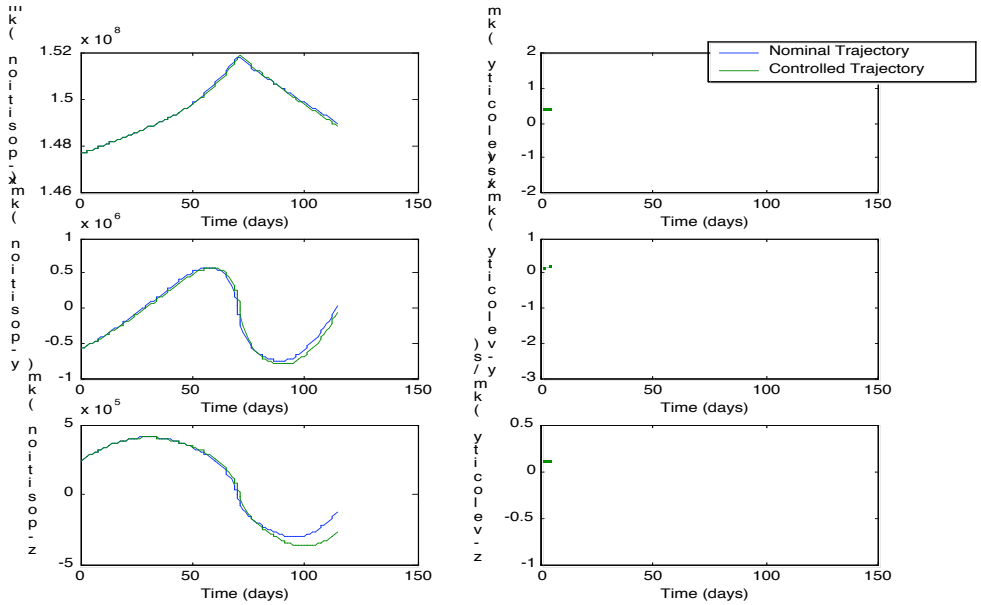

Figure 13: Nominal (solid) and Controlled (dotted) state trajectories for the "Late Departure" case.

Figure 14 shows the Correctability and the sail angles for the "New Technology" sailcraft, which uses the same sail as the other cases, but with a smaller total sailcraft mass (96 kg instead of 298 kg). As Figure 15 shows, the sailcraft is able to recover from much larger velocity errors (which occur during perigee) than in

any of the previous cases presented above. This occurs because the acceleration magnitude available to the sailcraft is larger due to the decreased total mass. In particular, note the relatively large Correctability near the end of the trajectory. Figure 15 demonstrates tracking of this trajectory in the presence of the system disturbances. The end-state error in the z-direction is once again larger than the end-state error in the other two directions. However, the z-position error remains very close to the nominal trajectory until just after the swingby of the Earth. It is the close proximity to the Earth where slight differences in position and velocity have large downstream effects that cause these large end-state errors. The controller does not reduce the state error to zero at these points and a very small error according to these plots (10^4 km) can be a full 10% closer to the Earth than was intended. This produces these large state errors downstream of the flyby.

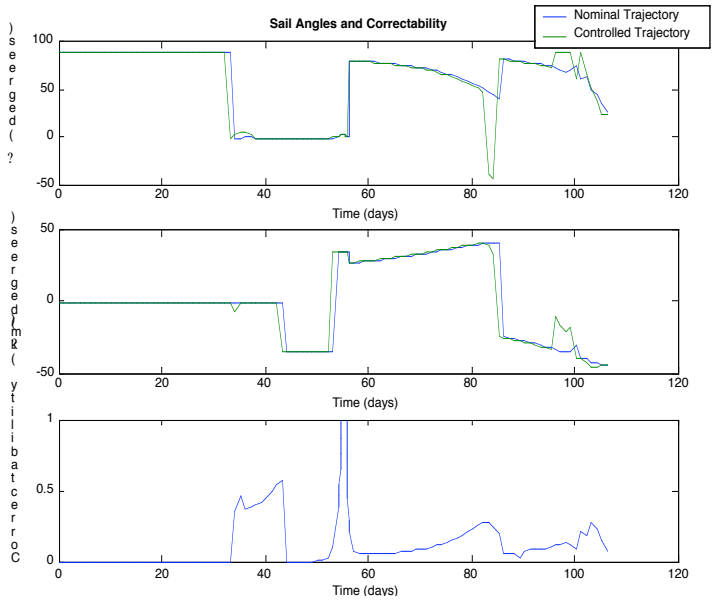

Figure 14: New technology sailcraft Correctability

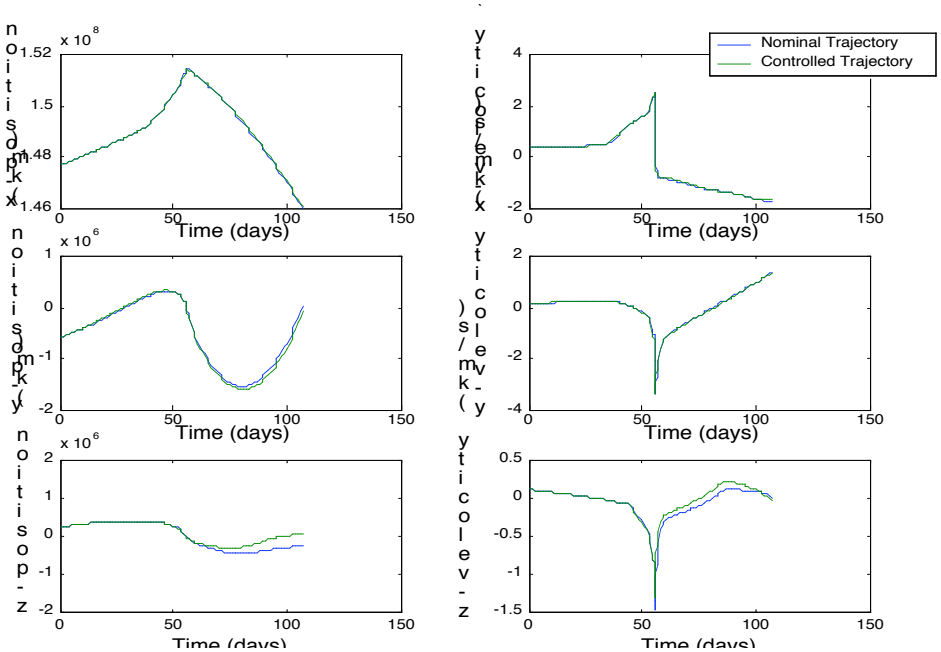

Figure 15: Nominal (solid) and Controlled (dotted) state trajectories for the "New Technology" case.

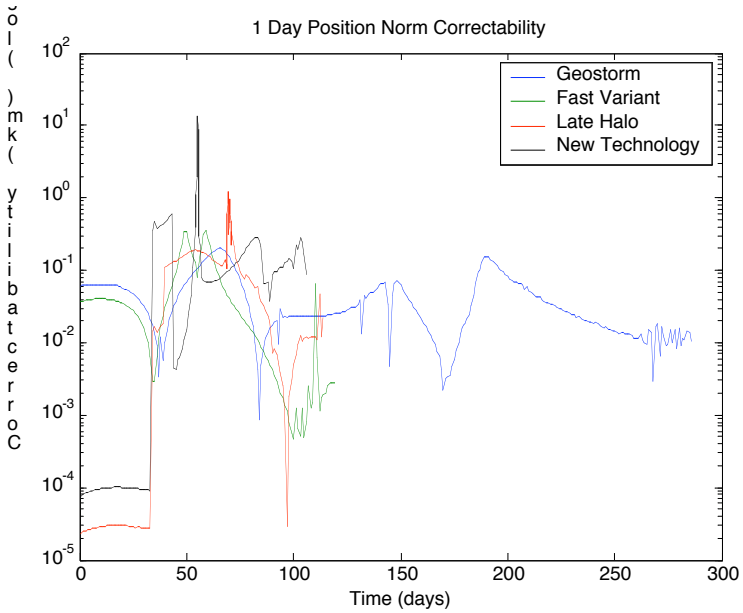

Figure 16: Correctability for all test cases

To directly compare Correctability, Figure 16 shows the position Correctability measures for all four trajectories on the same plot, using a log scale. While there are similar magnitudes and drop outs in Correctability in all three trajectories, the first flyby case (labeled fast in the figure) has significantly lower Correctability over a longer time interval than any of the other cases using the same sail. This region of poor Correctability occurs at the end of the trajectory when there is less time to recover from off-nominal errors. The "new technology" trajectory variant has higher Correctability than all of the other trajectories when it is nearing the target suggesting that it would handle the off-nominal errors better than the other three. This type of comparison may be useful in the early stages of mission design to weed out poorly-correctable trajectories before submitting them to full-fidelity Monte Carlo evaluation in an all-up spacecraft mission simulation.

Strategies for Sub-L1 Stationkeeping

The concept of solar sail stationkeeping comes from the sail trajectory options present in the circular-restricted case. In this case, the Earth's orbit is assumed to be perfectly circular and therefore the Earth-Sun synodic frame has constant Earth-position. In this case, the sailcraft can actually "sit" on an invariant manifold where the sail is positioned such that there is zero net acceleration acting on it. However, when the circular-restricted approximation is not made, there is no equilibrium in the synodic frame for the sailcraft to sit because the Earth is constantly moving along the Earth-Sun line.

However, it is possible to nearly fix the y and z position of the spacecraft in the synodic frame. The spacecraft moves in the synodic x-direction in concert with the Earth's movement along the Earth-Sun line. In order to determine what this "pseudo-hover" trajectory is, a method of successive approximations is used. The desired y and z equations are determined by the user (position is constant, velocity and acceleration are zero). With these determined, the position, velocity, and acceleration values for x are fed into a non-linear root-finder that uses the synodic acceleration equations to solve for the two sail angles and x-position. With this new approximation for the x-direction equations in hand, the process is repeated until the difference between approximations reaches a user-defined tolerance level.

While this process can reduce the x-error down to a certain tolerance level, it is impossible to eliminate the error entirely. This x-error also propagates into the y and z acceleration equations due to the centripetal acceleration and sail coupling terms present in the system model. So while the sailcraft can fly this hover for a period of time, it will deviate from the nominal as the approximation errors accumulate. In order to determine the final hover solution, closed-loop control is used to determine the trajectory that the sailcraft can actually fly. The approximated trajectory is used as the nominal trajectory and then the sailcraft uses

feedback control to fly this trajectory as close as possible. When this simulation is complete, the user has a pseudo-hover that the sail can fly with zero theoretical error.

With this process, the appropriate pseudo-hover trajectories were determined for the target end state (on the synodic x-axis, with zero synodic velocity) for each of the sail cases discussed above. The

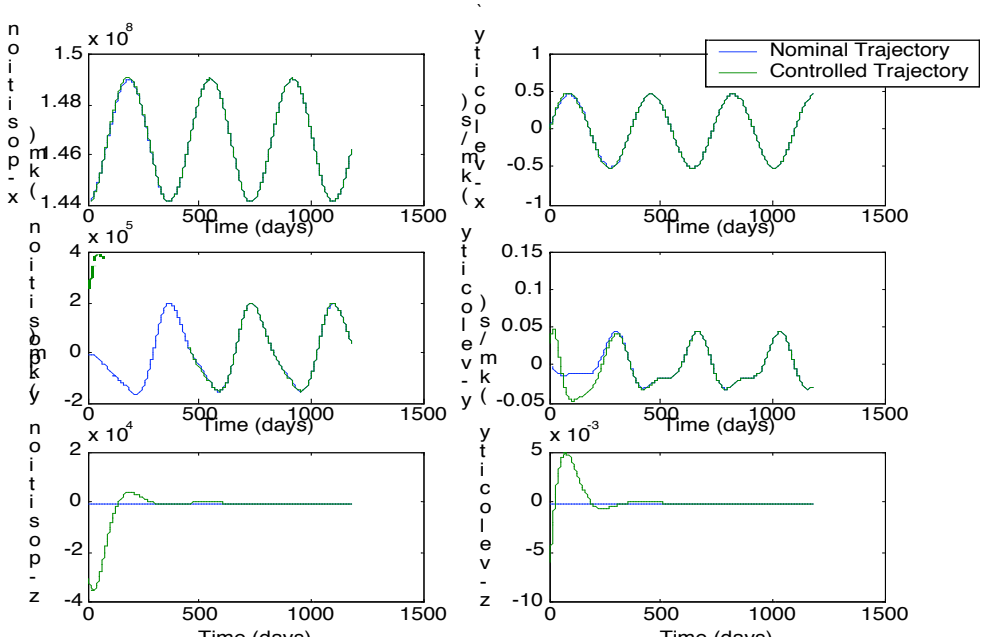

Figure 17: Pseudo-hover capture simulation for Geostorm Case

stationkeeping simulation was initialized, however, at the nominal end-state sailcraft position and velocity obtained in the transfer simulations above. The baseline Geostorm case had the smallest end-state error between nominal and target, and the results of capturing to the pseudo-hover trajectory from the Geostorm trajectory can be seen in Figure 17.

This plot demonstrates the sailcraft's ability (dotted line) to capture onto a periodic, pseudo-hover

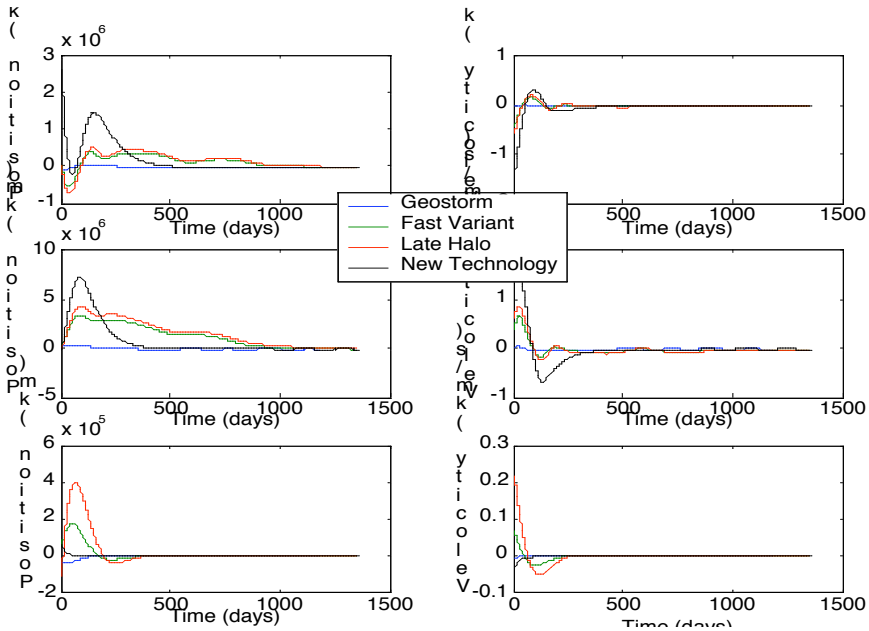

Figure 18: State error recovery for all test cases

trajectory (solid line. The initial errors in the x-direction are on the same order as the errors in the y-direction but are difficult to see because the variation in nominal x-position and velocity is an order of magnitude higher than the variation in the y-direction. This trajectory was simulated for 1,171 days or a little over three years. This pseudo-hover has a period equal to that of the Earth's orbital period.

This Geostorm case has an empirical 3% settling time of approximately one year (357 days). As the plot shows, the initial position and velocity errors were on the order of 10^5 km and 10^{-2} km/s respectively. When the faster transfer trajectories are used, the end-state errors are much larger and the system using the same controller takes much longer to capture to the nominal pseudo-hover. Figure 18 and Figure 19 show the state errors and the corrected sail angles, respectively, for the four test cases examined. The same linear quadratic controller cost function was used in all the pseudo-hover capture simulations.

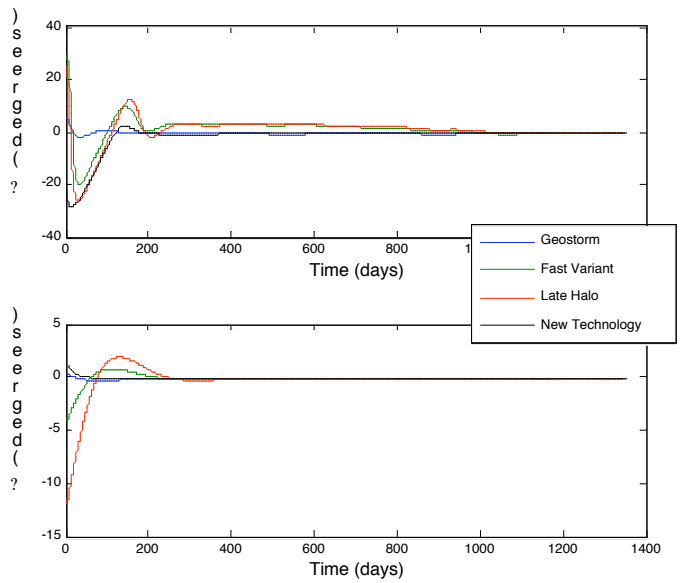

Figure 19: Capture simulation sail angles for all test cases

As Figure 18 shows, the initial state errors for the new technology case are much larger than the initial errors for the other three cases. Despite the increased size of the initial condition errors, the new technology case settles in approximately the same amount of time as the Geostorm case. On the other hand, the fast variant and late halo trajectories take approximately three years to settle to the same level.

This occurs because even though the sail is initially much farther off from the nominal trajectory than the fast and late halo variants, it is a much more correctable design. This benefit allows it to nullify these large initial condition errors in a much shorter time than the other sail designs were capable of. Figure 19 shows the corresponding sail angles for all four cases, indicating that the sail angles are much larger in the Fast and Late Halo variants, even though the trajectory errors remain large. Essentially, theses designs do not have sufficient control authority to effect a capture in reasonable times.

Conclusions

This work demonstrates the existence of a category of L1-to-sub-L1-region transfer trajectories, which have reduced travel time vs. the baseline Geostorm transfer trajectory, due to a gravitational assist from an Earth flyby along the trajectory. Three such L1-to-sub-L1 transfers with Earth flyby's were generated using a new sailcraft trajectory targeting and optimization tool, and compared in terms of the necessary sail control angle (cone and clock angle) histories. The cone angle maximum required excursion from zero was noted to be sensitive to the time of departing the initial L1 halo orbit; this is related to the sail-Sun-Earth geometry along the trajectory, and departing in a geometry when the Sun is "at the sail's back" is seen to be particularly beneficial, in terms of achievable transfer time (80 days) and maximum required cone angle (about 40 degrees). Trajectories with Earth flyby's, based on a sailcraft with baseline Geostorm mission materials and subsystem masses, are attainable with flight times that are about 1/3 of the L1-to-sub-L1 transfer time (286 days) baseline Geostorm mission. Also, a trajectory with Earth flyby, having a 73-day transfer time to a sub-L1 region twice as far away as the baseline Geostorm sub-L1 region, is found for a sailcraft based on updated materials and subsystem masses suggested in a paper by West.

The four trajectories considered have very different Correctabilities, making some more robust to disturbances along the trajectory. In particular, one of the Earth flyby cases exhibited poor Correctability near the end of the transfer from L1 to sub-L1, resulting relatively large sail angle excursions in a simulated correction control scenario compared to the other trajectories. Early application of a Correctability analysis may enable many alternatives to be examined early in the mission design cycle, eliminating the need for long simulations on cases that should not be pursued in detail.

In the cases considered, the faster transfer trajectories arrive with larger velocity, making them more difficult to capture into a stationkeeping orbit. The exception is the "New Technology" sailcraft, which is able to effect a capture due to its larger acceleration capability resulting from reduced mass. An indication of the acceptable "capture region" would be useful in the trajectory optimization process, so that end state weightings can be set to achieve feasible trajectories in this regard.

Acknowledgements

The research described in this paper was carried out at the Jet Propulsion Laboratory, California Institute of Technology, under a contract with the National Aeronautics and Space Administration. Also, the authors thank Dr. Chen-Wan Yen of JPL for providing the Geostorm baseline optimal reference trajectory and control profile used in these analyses.

References

1. Yen, C. W. "Solar Sail Geostorm Warning Mission Design." Paper AAS 04-107, presented at 2004 AAS/AIAA Spaceflight Mechanics Meeting, Maui, HI, Feb. 2004.
2. Sauer, C. G. "The L1 Diamond Affair." Paper AAS 04-278, presented at 2004 AAS/AIAA Spaceflight Mechanics Meeting, Maui, HI, Feb. 2004.
3. McInnes, C. *Solar Sailing – Technology, Dynamics and Mission Applications.* Springer Publications, 1999.
4. Ellis, J., et al, "A Solar Sail Integrated Simulation Toolkit." Paper AAS 04-283, presented at 2004 AAS/AIAA Spaceflight Mechanics Meeting, Maui, HI, Feb. 2004.
5. West, J. L. "The Geostorm Warning Mission: Enhanced Opportunities Based on New Technology." Paper AAS 04-102, presented at 2004 AAS/AIAA Spaceflight Mechanics Meeting, Maui, HI, Feb. 2004.
6. Tascione, T. F. Introduction to the Space Environment. Orbit Book Company, 1988. pp. 41-42, pg. 66, pg.100.
7. Bryson, A. E., and Y. C. Ho. Applied Optimal Control: Optimization, Estimation and Control. Hemisphere Publishing Co., 1975. pp. 225-228.
8. Lawrence, D. A., and S. Piggott, "Solar Sailing Trajectory Control for Sub-L1 Stationkeeping." Paper AIAA 2004-5014, presented at 2004 AIAA Guidance, Navigation and Control Conference and Exhibit, Providence, RI, Aug. 2004.
9. K. A. Seffen, G. T. Parks, and P. J. Clarkson, "Observations on the Controllability of Motion of Two-Wheelers", *Proc. Instn Mech. Engrs.*, Vol. 215, Part I, pp. 143—153, 2001.
10. T. Kailath, *Linear Systems,* Prentice-Hall, N.J., 1980.
11. M. Athans and P. L. Falb, *Optimal Control*, McGraw-Hill, N.Y., 1966.